

Modeling the FQHE from First Principles

M. L. Horner[†] and Alfred Scharff Goldhaber^{*}

[†]Southern Illinois University Edwardsville

^{*}C.N. Yang Institute for Theoretical Physics at State University of New York, Stony Brook

October 10, 2007

1 Abstract

Following the experimental discovery of the fractional quantum Hall effect (FQHE), Laughlin [1] gave an explanation and an ansatz for the many-body wave functions for the simple FQHE fractions. In a further advance Jain [2, 3, 4, 5] introduced the ‘composite fermion’ [CF] description to account for general fractions. We have a theory valid in quite a wide range, but it is tempting to ask for more: a deduction of FQHE from fundamental electromagnetic interactions. This might be one of those rare cases where rigorous deduction of the phenomena from the fundamental dynamics is within reach. We start by discussing some very simple adiabatic processes, and with these as motivation, discuss numerical models hinting at a pathway towards deducing FQHE. The crucial idea is that an electron in the presence of electric impurities and a strong magnetic field feels an induced magnetic field. Consider a two-dimensional Aharonov atom [6] in a uniform, perpendicular magnetic field. The attractive potential binding the electron to the (uncharged) ‘nucleus’ constrains the electron to occupy only degenerate states $m = 0$ or $m = 1$ of the lowest Landau level centered on the nucleus. For large separations of the atom and a concentrated charge, the $m = 0$ state of the atom will give the least overlap with the charge, and the lowest energy. However, at zero separation the $m = 1$ state will give the lowest energy. Because of mixing, the atom makes a transition within a diffuse ring of separation from the charge. The transition introduces an additional effective magnetic flux opposing the uniform magnetic field. We examine results from two generations of numerical models based on these concepts. First is a one-electron model in which all but one of the electrons involved in FQHE are treated as static “impurities”. This model generates half the CF downshift from applied to effective magnetic field. Second is a two-electron model testing which adds explicit anti-symmetrization of the paired state.

2 Models

To describe a single electron moving in two dimensions in a magnetic field, we use

$$H = \frac{1}{2} [\vec{\sigma} \cdot (\vec{p} - e\vec{A})]^2, \quad (1)$$

where

$$\hbar = c = m = 1 \quad (2)$$

and $\vec{\sigma}$ the Pauli spin matrices. This includes the interaction of the electron's spin with the magnetic field. Note that the lowest Landau level states are spin polarized, with energy $E = 0$. We choose the cylindrical gauge and assume the magnetic field B is strong enough that we may consider only the lowest Landau level and neglect mixing with higher levels. Our basis states have the form

$$\phi_m(z) = \frac{1}{\sqrt{\pi m!}} z^m e^{-zz^*/2} \quad (3)$$

where

$$z = x + iy = r e^{i\theta} \quad (4)$$

has been expressed in units of the magnetic length

$$\ell_B = \sqrt{2/eB}. \quad (5)$$

The magnetic length is both the root-mean-square radius of the $m = 0$ basis state and the radius of the area through which one quantum of magnetic flux, $\Phi_o = 2\pi/e$, passes. The total number of flux quanta passing through the system is then given by the squared radius of the system. That radius we take as the root-mean-square radius of the largest- m basis state.

The interactions among electrons are simplified to the interaction of one electron with fixed ‘‘impurities’’ representing the other electrons in the system. The mean density of the impurities, is

$$\rho \equiv \nu B, \quad (6)$$

where B is the flux density, i.e., the magnetic field strength measured in units of an Aharonov-Bohm quantum of magnetic flux. Because the impurities represent electrons, they have strong repulsive correlations. We implement this feature in our model via hard-shell repulsion among the otherwise randomly scattered impurities.

We construct each impurity of a pair of Gaussians,

$$V_n(z) = V_0 \left[\frac{1}{\alpha^2} e^{-|z-z_n|^2/\alpha^2} - \frac{1}{\alpha^2\beta^2} e^{-|z-z_n|^2/\alpha^2\beta^2} \right]. \quad (7)$$

The paired Gaussians give a system with zero average electrical potential and therefore a total energy $E = 0$, and approximate a repulsive charge screened by a compensating cloud (of course all in the presence of a uniform positive background charge representing the ions of the medium). The potential is the sum of the contributions from all of the impurities.

As a starting point for our parameter choices, we set $\beta^2 = 2$ so that the area computed from the root-mean-square radius of the negative shell would be twice that of the positive core, and then choose α so that plots of the density of states, participation ratio, and root-mean-square radius as a function of energy are approximately symmetric with respect to energy when there is one impurity for every two flux quanta. We vary both α and β to test the robustness of the model. In all cases, the widths of the Gaussians scale inversely with the square root of the impurity density, as we expect increased impurity density to increase localization of the individual impurities to minimize their overlap and hence their interaction energy. The potentials are constructed so that their space integrals are unchanged by this scaling. The impurities are randomly distributed, or randomly distributed with a minimum separation between adjacent impurity centers (hard-shell constraint), or placed on a hexagonal lattice. The centers of the impurities are required to lie within the disk, but their shape is unaffected by the disk boundary.

3 Single Particle Results

We consider energy spectra and compactness, \mathcal{C} , of states. The latter is defined by

$$\mathcal{C} = \sqrt{P}/R_{rms}. \quad (8)$$

The compactness measure uses the participation ratio, which measures the area of a state, [7, 8, 9],

$$P_\alpha = \frac{\left(\int d^2r |\Psi_\alpha|^2\right)^2}{\int d^2r |\Psi_\alpha|^4} = \left(\int d^2r |\Psi_\alpha|^4\right)^{-1}. \quad (9)$$

and the root-mean-square radius, which measures the width of the state,

$$R_{rms}^{(\alpha)} = \sqrt{\int d^2r r^2 |\Psi_\alpha|^2}. \quad (10)$$

Compactness measures the degree to which a state resembles a disk (most compact) or a ring (least compact). For a uniform disk, and densities corresponding to the $m = 0$ and $m = 1$ basis states, the ratio has exactly the value $\sqrt{2\pi}$. In the limit of large m , the states become more and more ‘ring-like’, and the value of the ratio tends towards zero.

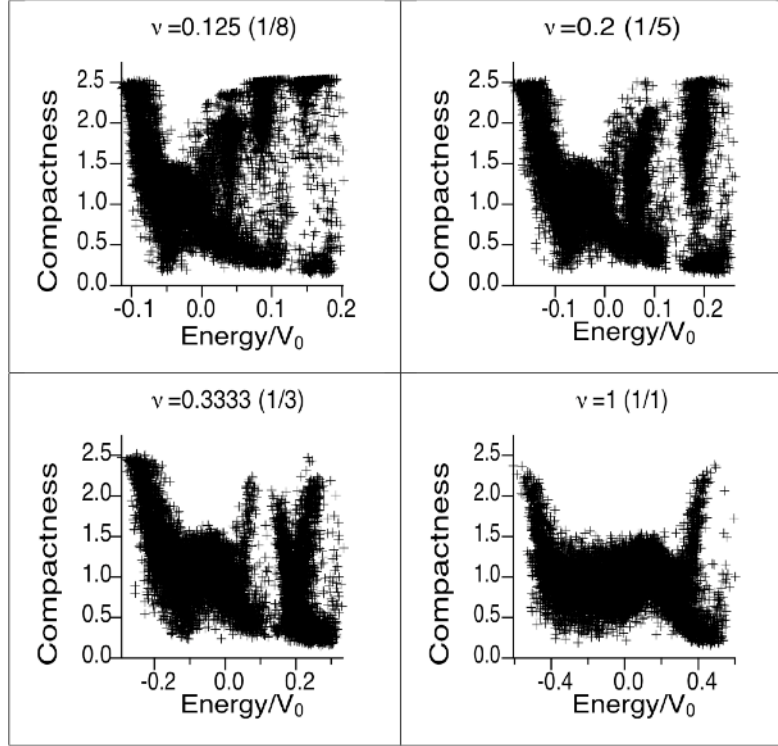


Figure 1: Combined distributions of eq.8 as a function of energy for ten different random distributions of impurities in the case of parameters set to $\alpha^2 = \frac{0.35}{\nu}$, $\beta^2 = 14.14$, minimum distance between centers of impurities is $0.70 \times (\text{System Size}/\sqrt{\#\text{Impurities}})$, using matrix elements up to 201 places from the diagonal and cross-terms in the participation function no more than 100 apart. The filling factor, ν is indicated at the top of each subfigure. Note the qualitative resemblance between compactness as a function of energy for $\nu = 1$ and that of the lower band for other values of ν . This is one of the indications that we are seeing an induced magnetic field.

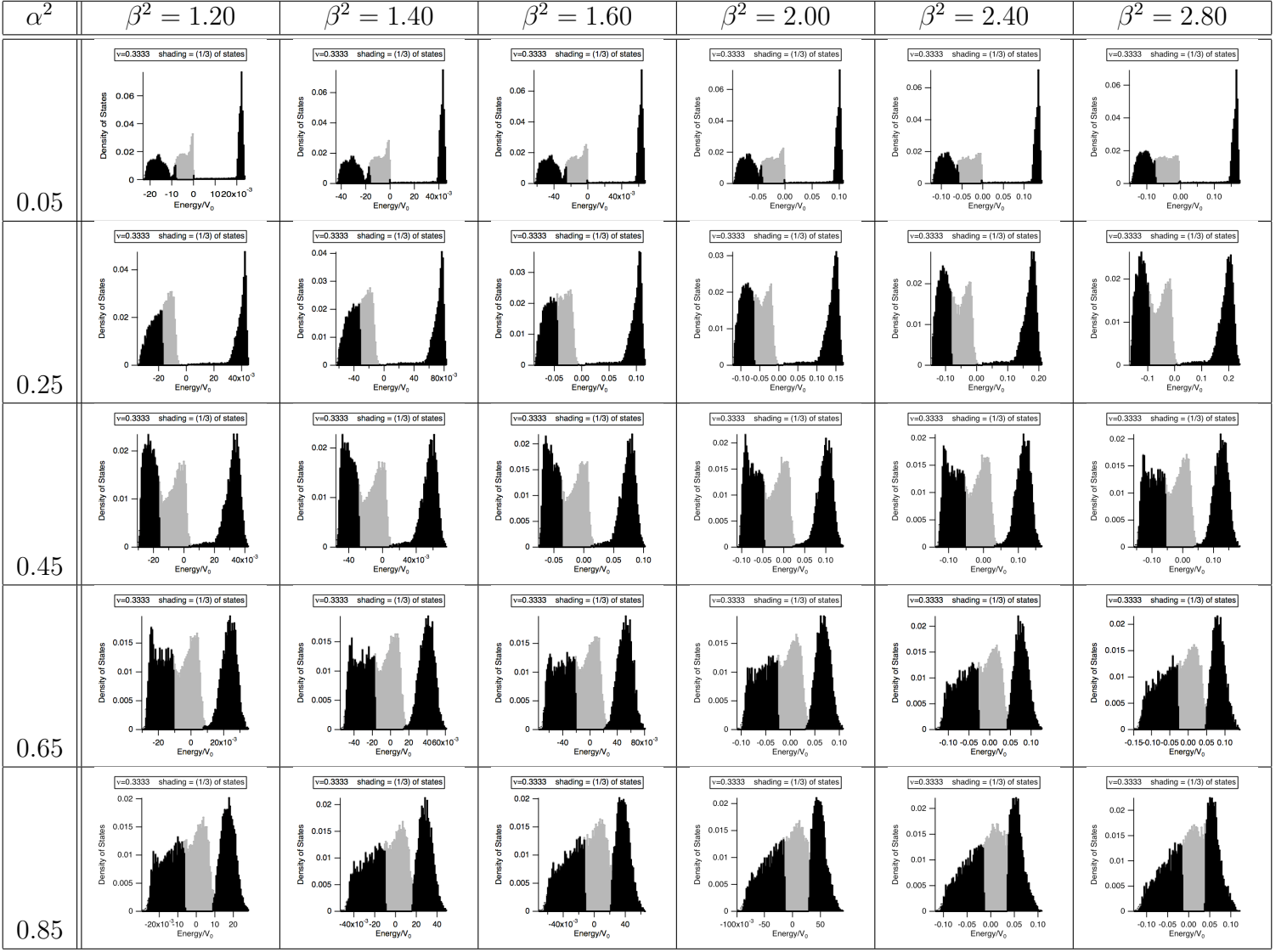


Figure 2: Energy histograms for randomly distributed impurities with hard-shell repulsion of 75%. This figure illustrates the robustness of our model with respect to input parameters. We are interested here in the gap between the highest energy and the other states. This is one of the indications that we are seeing an induced magnetic field. In addition, the location of the gap, ν of the states from the top counting down in energy, reveals that the magnetic field is shifted by half the amount predicted in CF theory.

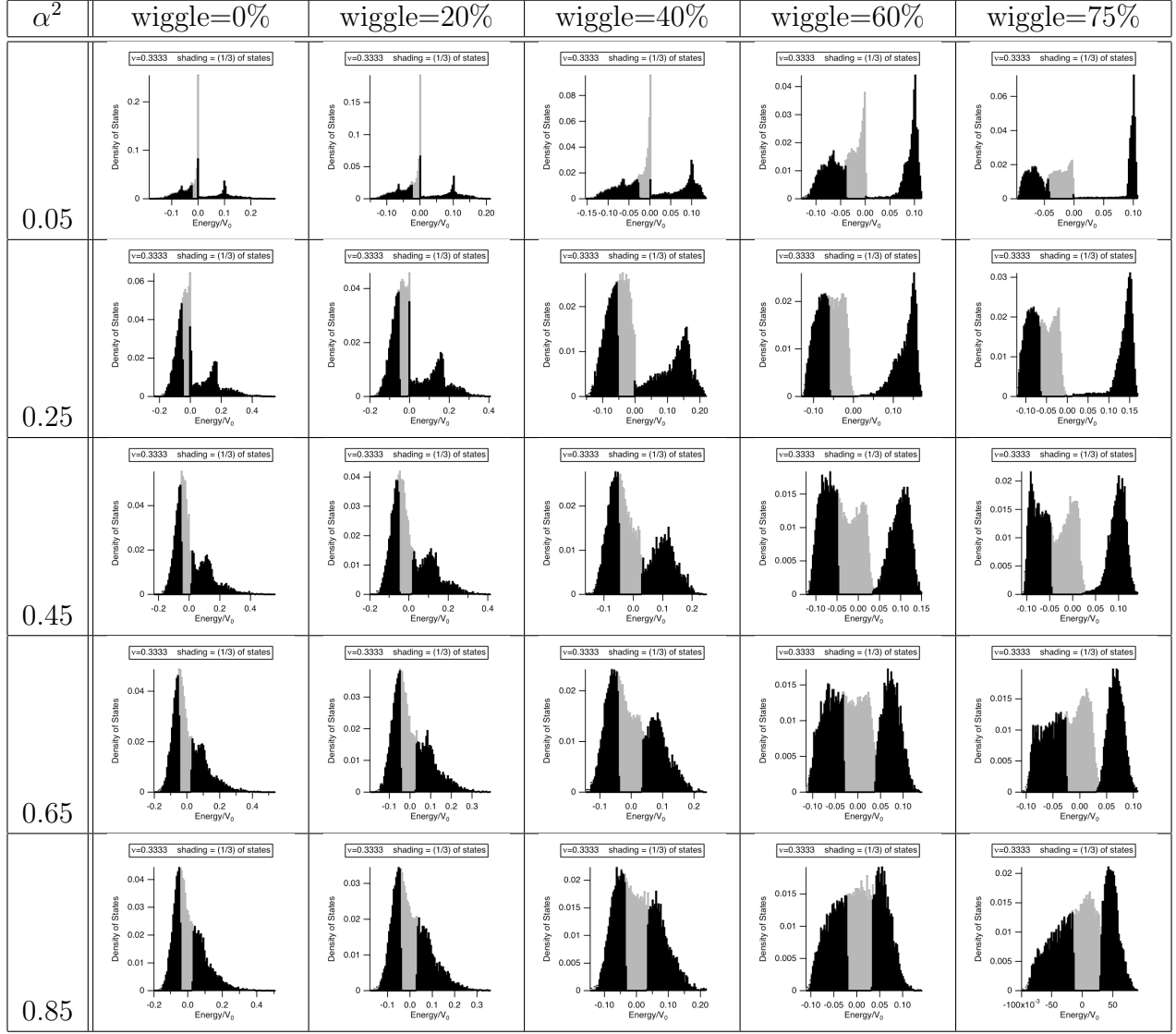


Figure 3: Energy histograms for randomly distributed impurities with varying sizes of the hard-shell repulsion. This figure further illustrates the robustness of our model with respect to input parameters. This is one of the indications that we are seeing an induced magnetic field. In addition, the location of the gap, ν of the states from the top counting down in energy, reveals that the magnetic field is shifted by half the amount predicted in CF theory.

4 Paired Particles

We extend the one particle treatment by combining single-particle states in an explicitly anti-symmetric way and by letting each single particle state interact with each impurity individually. This results in the matrix elements being given by the following integral

$$M(l, m; s, t) = \iint \left(\begin{array}{l} \left[\frac{(\vec{r}_1^*)^l e^{-|r_1|^2/2}}{\sqrt{\pi l!}} \frac{(\vec{r}_2^*)^m e^{-|r_2|^2/2}}{\sqrt{\pi m!}} - \frac{(\vec{r}_1^*)^m e^{-|r_1|^2/2}}{\sqrt{\pi m!}} \frac{(\vec{r}_2^*)^l e^{-|r_2|^2/2}}{\sqrt{\pi l!}} \right] \\ \times \left[\frac{e^{-|\vec{r}_1 - \vec{r}_n|^2/\alpha^2}}{\alpha^2} + \frac{e^{-|\vec{r}_2 - \vec{r}_n|^2/\alpha^2}}{\alpha^2} + \text{same with } \alpha \rightarrow \alpha\beta \right] \\ \times \left[\frac{(\vec{r}_1)^s e^{-|r_1|^2/2}}{\sqrt{\pi s!}} \frac{(\vec{r}_2)^t e^{-|r_2|^2/2}}{\sqrt{\pi t!}} - \frac{(\vec{r}_1)^t e^{-|r_1|^2/2}}{\sqrt{\pi t!}} \frac{(\vec{r}_2)^s e^{-|r_2|^2/2}}{\sqrt{\pi s!}} \right] \end{array} \right) d\vec{r}_1 d\vec{r}_2 \quad (11)$$

Numerical work to diagonalize this system is in progress.

5 Discussion

We have examined the energy spectra for the different kinds of distributions at impurity densities between 1 and 1100 impurities per 1000 magnetic flux quanta, for α^2 between 0.05 and 0.85, and for β^2 between 1.20 and 14.14. We find that for double Gaussian impurities randomly placed with a hard-shell constraint, the energy spectrum consists of a fraction $1 - n\nu$ of the states in the lowest energy band, and n higher energy bands each containing a fraction ν of the states. For the values of α and β we have explored, the splitting is generally reasonably clear when 60-70% of the system area is enclosed in the hard-shell regions. Narrower Gaussians, i.e., smaller values of α and β , show the split for smaller hard-shells than larger values do. Neither a random distribution nor a precise hexagonal close packing produces this type of energy spectrum. We also find that compactness as a function of energy for the lowest energy band is qualitatively similar to the single band that exists for one impurity per flux quantum. Both of these observations suggest that the lowest band should be considered a filled Landau level in a reduced magnetic field. According to [5], when the filling factor is given by

$$\nu = \frac{p}{2pq + 1}, \quad (12)$$

then the effective magnetic field is given by

$$B^* = B(1 - 2q\nu) \quad . \quad (13)$$

For ν in the interval $(1/3, 1/2)$, this means $q = 1$, for $(1/5, 1/4)$, $q = 2$, and for $(1/7, 1/6)$, $q = 3$.

As the single-particle model does not see the full shift in the magnetic field predicted in CF theory and does not distinguish even- and odd-denominator fractions, we are working on a model explicitly including antisymmetrization. Results of this work are not yet available.

References

- [1] R.B. Laughlin, Phys. Rev. Lett. **50**, 1395 (1983).
- [2] J.K. Jain, Phys. Rev. Lett. **63**, 199 (1989).
- [3] J.K. Jain, Phys. Rev. B **40**, 8079 (1989).
- [4] J.K. Jain, Phys. Rev. B **41**, 7653 (1990).
- [5] J.K. Jain, in: *Perspectives in Quantum Hall Effects*, edited by S. Das Sarma and A. Pinczuk (John Wiley and Sons, New York, 1997).
- [6] Y. Aharonov, S. Coleman, A.S. Goldhaber, S. Nussinov, S. Popescu, B. Reznik, D. Rohrlich and L. Vaidman, Phys. Rev. Lett. **73**, 918 (1994).
- [7] R.J. Bell and P. Dean, Discuss. Faraday Soc. **50**, 55 (1970).
- [8] J.T. Edwards and D.J. Thouless, J. Phys. C **5**, 807 (1972).
- [9] D.J. Thouless, Phys. Rep. **13C**, 93 (1974).